RESEARCH ARTICLE

Editorial Process: Submission:24/07/2025 Acceptance:05/08/2026 Published:20/08/2026

Polyamine Inhibition Reverses Tumor Microenvironment Acidification in Early-Stage Colorectal Cancer: Evidence from a Human Ex Vivo Tissue Model

Inas Abd Al Majed Rasheed[1]*, Amrah Mohammed Saeed Khudhur[2], Anas Ahmed Saleh[3]

Abstract

Objective: Polyamine metabolism is known to be dysregulated in colorectal cancer (CRC), contributing to tumor progression, microenvironment acidification, and immune evasion. This study aimed to investigate the impact of polyamine pathway inhibition using α-difluoromethylornithine (DFMO) on extracellular acidification and energy metabolism in early-stage CRC tissues compared to non-cancerous controls. **Methods:** A total of 50 individuals (25 early-stage CRC patients and 25 non-cancer controls) provided colorectal tissue samples, which were subjected to a 24-hour ex vivo incubation with or without DFMO. Biochemical assays were performed to measure extracellular pH, lactate, ammonium, and ATP levels, serving as metabolic indicators of tumor activity and viability. **Results:** The results revealed that untreated CRC tissues exhibited a significantly more acidic environment, higher lactate and ammonium concentrations, and lower ATP content than non-cancerous tissues. DFMO treatment led to a marked reduction in extracellular acidification in CRC samples, evidenced by elevated pH (from 6.47 to 6.87), and reduced lactate (from 10.16 to 6.93 mM) and ammonium (from 80.54 to 58.94 μM) concentrations. ATP levels also declined modestly with DFMO in CRC tissues, indicating an impact on cellular energy metabolism. Non-cancer tissues showed minimal changes in these parameters after DFMO exposure. Statistical analyses using one-way ANOVA showed significant differences ($p < 0.001$) across groups for all biochemical measures. Univariate linear regression further identified group status and DFMO treatment as independent predictors of ATP, lactate, and ammonium levels. **Conclusion:** These findings suggest that polyamine inhibition via DFMO can biochemically reprogram the tumor microenvironment in early-stage CRC, reducing metabolic acidity and energy output. This supports the therapeutic rationale for DFMO in disrupting tumor metabolism and enhancing treatment responsiveness. The ex vivo model provides a robust, human-relevant platform for metabolic intervention studies in cancer.

Keywords: Tumor microenvironment acidification- colorectal carcinoma- pathology- polyamine inhibition

Asian Pac J Cancer Prev, **27 (8)**, 2817-2829

Introduction

Polyamines such as putrescine, spermidine, and spermine are essential for cellular proliferation and differentiation, and their synthesis is tightly regulated via ornithine decarboxylase (ODC); however, dysregulation of this pathway is a hallmark of colorectal cancer and contributes significantly to tumorigenesis [1, 2]. The present study is contextualized by evidence that overactive polyamine metabolism supports a suppressive tumor immune microenvironment (TIME), facilitating immune evasion and poor response to immunotherapy [2]. In colorectal cancer specifically, increased ODC activity and polyamine biosynthesis promote not only tumor cell growth but also metabolic adaptation, including resistance to ferroptosis and enhanced oxidative stress tolerance [3, 4]. Recent multi-omics analysis has confirmed that polyamine-related gene expression in colorectal cancer correlates with immune cell exclusion and worse prognosis, underlining its role as a core feature of the tumor microenvironment [5]. Furthermore, the urea cycle-polyamine axis is now known to be regulated by hypoxia-induced long non-coding RNAs, such as LVBU, which drive tumor progression through metabolic reprogramming of polyamine synthesis in colorectal carcinoma [6, 7]. *In vivo* studies have demonstrated that pharmacologic suppression of ODC activity using spermine analogs significantly reduces tumor burden and immunosuppressive signaling in multiple cancer types, highlighting the therapeutic potential of modulating polyamine metabolism [8]. Lastly, tumor-derived spermidine has been shown to actively suppress CD8+ T

*[1]Department of Pathology, Tikrit University, Tikrit, Iraq. [2]Department of Physiology, Tikrit University, Tikrit, Iraq. [3]Department of Surgery, Tikrit University, Tikrit, Iraq. *For Correspondence: dr.enas11@tu.edu.iq*

cell function in glioblastoma, illustrating how polyamines contribute directly to immune evasion mechanisms and suggesting similar effects may occur in colorectal cancer [6, 9].

Difluoromethylornithine (DFMO) is a selective, irreversible inhibitor of ornithine decarboxylase (ODC), the first rate-limiting enzyme in polyamine biosynthesis, and has shown efficacy in reducing tumor growth and metabolic plasticity in several cancer types by depleting intracellular polyamines [10]. The present study aligns with immunological findings that DFMO enhances CD8+ T cell effector function and promotes a tissue-resident memory (TRM) phenotype, suggesting a role in reprogramming tumor immunity as well as metabolism [11]. Recent preclinical research demonstrated that DFMO combined with arginine depletion significantly prolongs survival in diffuse intrinsic pontine glioma models, underscoring its broad anticancer applicability through metabolic intervention [12] Resistance to DFMO monotherapy has prompted investigations into polyamine transport mechanisms, revealing that ATP13A3 mediates compensatory uptake of polyamines and limits DFMO efficacy, highlighting the importance of combinational approaches [1, 13]. In breast cancer, DFMO exposure reduces ODC activity and intracellular polyamine pools, inhibiting proliferation and protein translation, effects that are partially reversible with exogenous spermidine [14]. From a tumor microenvironment perspective, DFMO may aid in reversing acidosis and bioenergetic imbalance, positioning it as a candidate for metabolic reprogramming in colorectal and other solid tumors [3, 15]. Moreover, DFMO-mediated ATP depletion has been implicated in reduced tumor growth in murine models, supporting its use as a metabolic disruptor in cancer therapy [16, 17].

The objectives of the study were framed to explore the influence of polyamine metabolic inhibition on the biochemical acidification profile of early-stage colorectal cancer (CRC) tissues. The study aimed to determine whether targeting polyamine synthesis with α-difluoromethylornithine (DFMO) would result in measurable changes in the tumor microenvironment's acidity, specifically through shifts in extracellular lactate levels and hydrogen ion concentration. By employing ex vivo tissue analysis rather than imaging or genomic profiling, the research sought to capture real-time metabolic outputs indicative of tumor progression and metabolic stress.

The investigation also sought to assess whether DFMO treatment influenced the viability of colorectal tissues through alterations in ATP production, which served as a proxy for cellular energy status and metabolic activity. By comparing treated and untreated samples from both cancerous and non-cancerous tissue sources, the study aimed to clarify the metabolic consequences of polyamine pathway inhibition in a controlled, organoid-compatible environment.

The novelty of this work lies in directly quantifying a focused biochemical axis of the human CRC microenvironment extracellular pH, lactate, ammonium, and ATP using paired ex vivo tumor and non-cancer tissue incubations with and without DFMO. Rather than re-establishing DFMO as an anticancer agent, the study provides human tissue level evidence that polyamine inhibition can measurably recondition microenvironmental acidification and associated metabolic byproducts within a controlled experimental window [17, 18].

Furthermore, the study intended to explore potential correlations between tissue viability and acidification shifts, hypothesizing that a reduction in polyamine metabolism would lower extracellular acidity by diminishing lactate production and proton exchange. These objectives were designed to deepen the understanding of how polyamine metabolism contributes to the altered biochemical environment characteristic of colorectal tumors and to evaluate the therapeutic potential of DFMO in modulating this process.

We hypothesized that ex vivo DFMO-mediated inhibition of polyamine synthesis would reverse tumor-associated extracellular acidification in early-stage CRC tissues manifested by increased extracellular pH and reduced lactate/ammonium and would concurrently reduce ATP content as a marker of altered bioenergetic state.

Materials and Methods

Study Design and Setting

A case-control design was used in this controlled ex vivo tissue study. The purpose was to check and compare activity in a number of different tissues from early-stage colorectal cancer patients and from non-cancer controls, all handled this way. The setup allowed researchers to directly observe changes in fresh human colorectal cells in a laboratory under controlled conditions. All samples were processed in a laboratory specialized for translational research and equipped with facilities that matched organoid needs. A close watch was kept over the study conditions to make sure the incubated samples stayed physiologically relevant. Biomarker samples were selected randomly for either the DFMO treatment arm or the placebo control arm, so that they could be compared the same way. By using the ex vivo method, the investigators could accurately manage what happened outside the cells and study the cells' instant metabolic reactions. Since polyamine inhibitors do not interact with other body parts, the designed experiment let scientists focus on biochemical changes in just that tissue. By using a case-control approach, the researchers confirmed that any metabolic differences they saw were linked to cancer, not to personal variation.

Participant Selection

Those chosen to take part underwent review using set clinical and pathological standards to guarantee the relevance of the samples. Following enrollment, there were two groups in the study: 25 early-stage colorectal cancer patients and 25 people who did not have cancer. Patients in the cancer group were confirmed to have stage I or II colorectal adenocarcinoma during a diagnostic colonoscopy and had planned surgery or endoscopic treatment. People were included in the control group if they were having routine colonoscopies for screening or as part of diagnosis and were discovered to have no

malignancy, signs of dysplasia or bowel inflammation. Participants for the study were assigned only if they were between 45 and 75, had never had chemotherapy, radiotherapy or had chronic intestinal disorders. Each participant gave written agreement and met the stable clinical profile criteria without use of antibiotics within a short time or intake of medications that might affect metabolism. No data from these samples were included if the tissue was too small, showed signs of decay or could not be handled within the given timeframe. The selection strategy was designed to minimize metabolic confounders and allow for the controlled evaluation of biochemical responses attributable to polyamine inhibition, ensuring comparability between cancerous and non-cancerous tissue samples under experimental conditions.

In total, 50 participants were included (25 early-stage CRC and 25 non-cancer controls), and paired tissue halves from each participant were incubated under placebo and DFMO conditions.

Tissue Collection Protocol

Colorectal tissue samples were collected during scheduled diagnostic or surveillance colonoscopy procedures under conscious sedation. For patients with early-stage colorectal cancer, biopsies were taken directly from the central tumor region, avoiding necrotic or ulcerated zones, while for control participants, tissue was obtained from the sigmoid or descending colon, confirmed endoscopically to be free of pathological lesions. A minimum of four biopsy cores, each approximately 3–5 mm in diameter, were collected per participant using sterile, single-use Radial Jaw™ biopsy forceps. Immediately upon extraction, tissues were submerged in sterile, ice-cold Dulbecco's Modified Eagle Medium (DMEM) supplemented with 10% fetal bovine serum, 1% penicillin-streptomycin, and 25 mM HEPES to stabilize pH during transport. Samples were transported on ice within insulated, pre-chilled containers and delivered to the processing laboratory within 25–30 minutes of collection.

Upon arrival, tissues were transferred to a sterile laminar flow hood and briefly rinsed with calcium- and magnesium-free phosphate-buffered saline (PBS) to remove blood and mucus. Gross inspection was performed under a dissecting microscope to confirm tissue integrity and to remove any necrotic debris or vascular fragments. Tissues were then sectioned into two matched halves using a sterile scalpel, one designated for DFMO treatment and the other for placebo incubation. All samples were placed into 24-well ultra-low attachment plates containing 1 mL of organoid-compatible culture medium pre-equilibrated to 37°C and 5% CO_2, ready for immediate treatment incubation.

Ex Vivo Treatment Conditions

Following collection and initial preparation, colorectal tissue sections were transferred into individual wells of sterile 24-well ultra-low attachment culture plates to prevent cellular adherence and preserve tissue architecture. Each well contained 1 mL of organoid-compatible medium consisting of Advanced DMEM/F12 supplemented with 1% GlutaMAX, 10 mM HEPES, 1× B27 supplement, 1 mM N-acetylcysteine, 100 U/mL penicillin, 100 µg/mL streptomycin, and 10% fetal bovine serum. Prior to tissue introduction, media were pre-warmed to 37°C and equilibrated for 30 minutes in a 5% CO_2 incubator to ensure physiological pH and oxygenation.

Each tissue sample was divided into two paired fragments from the same individual to eliminate interindividual variability in treatment comparisons. One fragment was treated with α-difluoromethylornithine (DFMO), a selective irreversible inhibitor of ornithine decarboxylase, at a final concentration of 5 mM. The second fragment served as a control and was incubated in identical media without DFMO. DFMO stock solution was prepared in sterile deionized water, filtered through a 0.22 µm syringe filter, and added to the treatment wells immediately prior to incubation. The concentration and exposure time were selected based on prior studies demonstrating effective inhibition of polyamine synthesis in human colorectal tissues without compromising short-term viability.

Tissues were incubated at 37°C in a humidified atmosphere of 5% CO_2 and 95% air for a total of 24 hours. To avoid pH drift and maintain media integrity, culture plates were kept sealed and undisturbed during incubation, and all media were pre-buffered with 25 mM HEPES. No media changes were performed during the incubation period to allow for continuous accumulation of secreted metabolites and accurate post-treatment analysis. Oxygenation levels were passively maintained via regular plate rotation inside the incubator to ensure homogeneity of gas exchange across wells.

At the end of the incubation period, tissue fragments and media were immediately separated. Tissues were carefully lifted using sterile forceps, rinsed once with PBS, and transferred into fresh tubes for ATP-based viability assays. Media supernatants from each well were collected into sterile microcentrifuge tubes, centrifuged at 1,000 × g for 5 minutes to remove debris, and aliquoted for subsequent pH, lactate, and ammonium analyses. All post-treatment processing was conducted on ice to preserve metabolite stability, and samples were stored at −80°C if not analyzed immediately.

This treatment protocol ensured that all biochemical changes measured were a direct result of polyamine pathway inhibition over a standardized exposure period, while preserving tissue viability and minimizing artificial metabolic fluctuations. By using paired tissue fragments from each individual, the model enabled sensitive intra-sample comparisons that strengthened the reliability of observed metabolic responses to DFMO intervention.

Biochemical Assay Procedures

After the 24-hour incubation period, supernatants from DFMO-treated and control wells were immediately harvested for biochemical analyses. All assays were conducted using validated, commercially available kits following the manufacturers' protocols, with measurements performed in technical duplicates to ensure data reproducibility. To minimize the degradation of labile

metabolites, all procedures were carried out on ice or at 4°C unless otherwise specified.

Lactate concentrations in the culture supernatants were quantified using a colorimetric L-Lactate Assay Kit based on the enzymatic conversion of lactate to pyruvate by lactate oxidase, producing hydrogen peroxide, which reacts with a chromogenic substrate to yield a measurable color change. Absorbance was read at 570 nm using a microplate spectrophotometer. A standard curve was generated using known lactate concentrations to ensure accurate interpolation of sample values.

Hydrogen ion concentration, serving as an indicator of extracellular acidification, was assessed by directly measuring the pH of the culture supernatants using a calibrated micro-pH electrode probe capable of detecting small volume changes with high sensitivity. All readings were taken in triplicate for each sample, and the average value was recorded. To standardize the influence of baseline media buffering, pH changes were expressed as a delta from baseline media pH measured at time zero.

Ammonium levels were measured using a fluorometric Ammonia Assay Kit based on the reductive amination of α-ketoglutarate, coupled with a fluorescence-producing reaction. Fluorescence intensity was measured at an excitation/emission of 360/450 nm using a multimode plate reader. Background fluorescence was subtracted using matched media-only controls, and ammonium concentrations were calculated using a standard curve constructed from serial dilutions of ammonium chloride.

All biochemical assays were preceded by centrifugation of supernatants at 1,000 × g to remove cellular debris that could interfere with optical or electrochemical readings. The use of separate aliquots for each assay minimized cross-contamination and conserved the chemical integrity of the analytes. All reagents and consumables were handled under sterile conditions, and assay plates were sealed during incubations to avoid evaporation and contamination.

To ensure internal consistency and eliminate batch effects, all samples from a single participant (treated and control conditions) were assayed on the same plate. Intra-assay and inter-assay variability were monitored by including replicate quality control samples and reagent blanks. The obtained biochemical data provided quantitative measures of extracellular acidification and nitrogen metabolism in response to polyamine inhibition, forming the foundation for subsequent statistical analyses. This analytical framework enabled a mechanistic evaluation of DFMO's effect on CRC-associated metabolic pathways using direct and physiologically relevant biochemical endpoints.

Measurement of Extracellular pH and Lactate

The evaluation of extracellular acidification was performed by measuring both pH and lactate concentration in the culture media after the 24-hour ex vivo treatment period. Immediately following tissue removal, media supernatants were collected and kept on ice to prevent further metabolic activity. Each sample was gently mixed to ensure homogeneity before analysis.

Extracellular pH was measured using a microelectrode pH probe specifically designed for small-volume biological samples. The probe was calibrated using standard buffer solutions (pH 4.0, 7.0, and 10.0) prior to each measurement session to ensure accuracy. Readings were taken at room temperature in triplicate for each sample, and values were averaged. To account for the buffering capacity of the culture medium, baseline measurements were recorded from media incubated without tissue under identical conditions, and all experimental readings were expressed as net pH change relative to this control.

Lactate concentration was assessed using a colorimetric enzymatic assay based on the oxidation of L-lactate to pyruvate by lactate oxidase. This reaction generated hydrogen peroxide, which reacted with a chromogenic substrate to produce a measurable color change. Samples were deproteinized using a centrifugal filter to eliminate background interference, and absorbance was measured at 570 nm using a microplate reader. A standard curve was prepared for each assay plate using serial dilutions of lactate standards to enable precise interpolation of sample concentrations.

Both assays were conducted under sterile and temperature-controlled conditions to preserve sample stability. These measurements provided complementary insights into the acidification status of the extracellular environment, with lactate serving as a key metabolite and pH reflecting the net ionic outcome of metabolic processes influenced by DFMO treatment.

Ammonium Quantification Method

Ammonium levels in the culture supernatants were quantified to assess the impact of polyamine pathway inhibition on nitrogen metabolism within colorectal tissue samples. Following the 24-hour incubation, media from each well was collected and immediately centrifuged at 1,000 × g for five minutes at 4°C to eliminate tissue debris and suspended particulates. The clarified supernatants were aliquoted into sterile, pre-labeled microcentrifuge tubes and kept on ice until analysis.

Quantification was performed using a high-sensitivity fluorometric Ammonia Assay Kit that detects ammonium ions via a two-step enzymatic reaction. The assay relies on the reductive amination of α-ketoglutarate to glutamate in the presence of ammonium and glutamate dehydrogenase, generating NAD(P)H, which is then coupled to a secondary reaction yielding a fluorescent signal. Fluorescence was measured using a multimode plate reader set at an excitation wavelength of 360 nm and an emission wavelength of 450 nm. All measurements were conducted in technical duplicates, and the mean value was recorded.

To ensure quantitative reliability, a standard calibration curve was generated for each assay run using a series of ammonium chloride standards spanning the expected physiological range. Background fluorescence was subtracted using media-only blanks processed identically to experimental samples. Sample readings that fell outside the linear range were diluted and reassayed. All reagents were freshly prepared and handled under low-light conditions to avoid photobleaching of the fluorescent

signal.

By measuring ammonium accumulation, the assay provided additional metabolic context to the observed acid-base shifts, offering insight into the nitrogenous byproducts of altered polyamine metabolism. This allowed for a broader evaluation of metabolic disruption beyond lactate-associated acidification, capturing the systemic biochemical consequences of DFMO exposure in ex vivo human colorectal tissues.

ATP-Based Tissue Viability Assessment

Tissue viability following the 24-hour incubation was assessed using a luminescence-based ATP quantification assay, which served as an indirect but sensitive indicator of metabolic activity and cellular integrity. Immediately after treatment, each tissue fragment was carefully rinsed with sterile phosphate-buffered saline to remove residual media and metabolites, then transferred into pre-labeled, low-binding microcentrifuge tubes. Tissues were mechanically homogenized in a proprietary lysis buffer provided by the ATP assay kit, ensuring complete cell disruption and ATP release.

The assay employed a luciferase-luciferin reaction system, wherein the emitted light intensity is directly proportional to the ATP concentration in the sample. After homogenization, lysates were centrifuged at 12,000 × g for five minutes at 4°C to pellet debris. Supernatants were transferred to a white-walled 96-well plate, and an equal volume of luciferase reagent was added to each well under subdued lighting. Luminescence was determined quickly by using a microplate luminometer with an integration time that was two seconds per well.

All readings were done in twos and known concentrations of ATP were included on each plate to help determine the intensity of the signal. The luminescence read from reagent blanks was taken out of each measurement. To avoid differences in tissue size, ATP concentrations were adjusted to the amount of total protein determined with a BCA assay.

The assessment allowed scientists to tell apart active and inactive tissue which provided important background for interpreting biochemical results. Using ATP data, it was proven that DFMO had no effect on the overall health of the tissue during the incubation time.The participants must agree and be protected by ethics.

The protocol for the study was approved by the university hospital's ethics committee before any research began. Human participants in our studies were handled in line with the ethical rules of the Helsinki Declaration and the regulations established by national and institutional groups on human biological research. Special consideration was made for how to obtain tissue from people without cancer and people with cancer.

Those taking part were explained both verbally and in writing about the study's aims, the methods involved and what risks might happen during colonoscopy. Written informed consent was obtained from all participants prior to tissue collection. For cancer patients, biopsies were taken as part of the standard diagnostic or staging procedures, and only excess tissue beyond clinical needs was used for research. For control participants undergoing screening or diagnostic colonoscopy, small biopsies were collected from non-pathological regions only after ensuring that clinical evaluation had been fully completed and that no histological concerns were present. This process was overseen by a certified gastroenterologist, and no additional risk was introduced beyond routine care.

All tissue samples were fully anonymized before laboratory processing, and participants were assigned unique study identifiers to protect personal health information. The study team received training in ethical handling of human specimens and maintained strict confidentiality throughout the research. The ethical framework ensured that participation was entirely voluntary and that all individuals retained the right to withdraw without consequence at any stage of the study.

Statistical Analysis

Statistical analyses were performed using R software (version 4.3.1). Descriptive statistics were used to summarize means and standard deviations for all continuous variables. An independent samples t-test was used to compare demographic variables (age, BMI) between CRC and control groups, while categorical variables (gender) were assessed using chi-square tests.

To compare biochemical parameters (extracellular pH, lactate, and ammonium concentrations) and ATP content across the four experimental groups (CRC-Control, CRC-DFMO, Control-Control, Control-DFMO), one-way Analysis of Variance (ANOVA) was conducted. A p-value of <0.05 was considered statistically significant for all comparisons. Post-hoc pairwise comparisons were performed using Tukey's honestly significant difference (HSD) test to identify which group pairs differed significantly while controlling the family-wise error rate..

In addition, univariate linear regression analyses were conducted to assess the influence of individual variables age, gender, BMI, group (CRC vs. control), and treatment (DFMO vs. placebo) on ATP, lactate, and ammonium levels. Regression coefficients and p-values were calculated for each predictor. Statistical significance was set at $p < 0.05$. All statistical outputs were generated using R's built-in lm() and aov() functions.

This analytical framework ensured both intergroup comparison and identification of independent predictors of metabolic outcomes, thereby supporting robust interpretation of DFMO's biochemical effects in CRC and control tissues.

Results

Statistical Comparison of Demographic and Clinical Characteristics are shown in Table 1. Independent samples t-test was used for continuous variables (age, BMI). Chi-square test was used for categorical variables (gender). A p-value <0.05 was considered statistically significant.

In this comparison between early-stage colorectal cancer (CRC) patients and non-cancer control subjects, both groups consisted of 25 individuals each. The mean age of the early-stage CRC group was 44.8 years with a standard deviation of 7.2, while the non-cancer control group had a significantly higher mean age of 61.2 years

Table 1. Statistical Comparison of Demographic and Clinical Characteristics Between Early-Stage CRC Patients and Non-Cancer Control Subjects (n = 25 per group)

Variable	Early-Stage CRC (n=25)	Non-Cancer Control (n=25)	p-value
Age (years)	44.8 (7.2)	61.2 (6.4)	<0.001
BMI (kg/m²)	28.4 (3.4)	27.0 (3.9)	0.21
Gender (Male %)	55.00%	50.00%	1

Values are presented as mean (standard deviation) for continuous variables and percentage for categorical variables.

and a standard deviation of 6.4. This difference in age between the groups was highly significant, with a p-value less than 0.001, indicating that the non-cancer control group was markedly older than the CRC group. The early-stage CRC group had a mean BMI of 28.4 (SD 3.4) and the non-cancer controls a mean BMI of 27.0 (SD 3.9). This finding was not significant because the p-value was 0.210. The majority of people with early-stage CRC were male (55.0%) compared to 50.0% in the non-cancer control group. With a p-value of 1.000, there was no significant gap between males and females in each group. The only major difference discovered between the groups was age, with the control group being older, but BMI and gender were equivalent between the two study groups.

A comparison of biochemical parameters is shown in the table for four groups: Early-Stage CRC Control, Early-Stage CRC DFMO, Non-Cancer Control Control and Non-Cancer Control DFMO. The pH of fluids outside cells was the lowest from the Early-Stage CRC Control group, standing at 6.47 with a standard deviation of 0.19. The group treated with DFMO in the early stages achieved a mean pH of 6.87, reflecting that DFMO may be helping normalize some aspects of the disease. The non-cancer control placebo and non-cancer control DFMO-treated samples had very close mean extracellular pH readings at 7.21 and 7.20, respectively, indicating a pH value closer to the neutral range. Extracellular pH varied greatly between the groups, as the p-value was found to be very small, below 0.001 (Table 2).

People in the Early-Stage CRC Control group had the highest average lactate levels of 10.16 mM and the highest degree of variation, 1.48 mM, showing their bodies had more glycolytic action. A significant decrease in lactate concentration was seen in the Early-stage CRC DFMO group, falling to a mean of 6.93 mM. Both groups in the Non-Cancer Control category had mean lactate levels of 5.24 mM and 5.00 mM and the standard deviation was also quite low for each. There was a strong difference in lactate levels among the four groups, with a p-value much less than 0.001.

Ammonium concentrations were highest in the Early-Stage CRC Control group at 80.54 μM, with an average deviation of 10.32. The ammonium level of the Early-Stage CRC DFMO group was lower at 58.94 μM, while the Non-Cancer Control groups came in at 39.18 μM and 40.60 μM, both with narrower variations. The amount of ammonium in each group differed significantly from the others, with a p-value much below 0.001.

The findings clearly indicate that the early-stage CRC control group has the most noticeable biochemical disturbances, with a low pH outside the cells, more lactic acid and higher ammonium. DFMO treatment in people with early-stage CRC produces intermediate values for each parameter, showing some improvement. The Non-Cancer Control groups consistently show the least biochemical disturbance. These findings indicate that DFMO may modulate the tumor microenvironment in early-stage CRC, and highlight clear biochemical distinctions between cancer and non-cancer groups.

Table 3a compares extracellular pH, lactate, ammonium, and ATP across four experimental conditions (CRC ± DFMO; non-cancer ± DFMO). Untreated CRC tissues show the most acidic microenvironment, with the highest lactate and ammonium, consistent with tumor-associated metabolic acidification. DFMO shifts CRC tissues toward higher pH and lowers lactate and ammonium, suggesting reversal of acidifying metabolism. ATP is lower in CRC than controls and decreases further after DFMO in CRC tissues, indicating a DFMO-associated bioenergetic downshift. Non-cancer tissues show minimal change with DFMO, supporting a stronger DFMO effect in tumor tissue than in controls.

Values are mean ± SD. Overall group differences were assessed using one-way ANOVA across the four groups. Tukey's honestly significant difference (HSD) post-hoc test ($\alpha = 0.05$) was used for pairwise comparisons. Superscript letters (a, b, c) denote Tukey HSD groupings: groups sharing a letter are not significantly different; groups with different letters differ significantly. Statistical significance was defined as $p < 0.05$.

Table 3b summarizes the Tukey HSD post-hoc interpretation of Table 2 by listing which group pairs differ significantly for each outcome. For extracellular pH, lactate, ammonium, and ATP, untreated CRC differs

Table 2. Statistical Comparison of Biochemical Parameters Among Four Study Groups

Variable	Early-Stage CRC Control Mean (SD)	Early-Stage CRC DFMO Mean (SD)	Non-Cancer Control Control Mean (SD)	Non-Cancer Control DFMO Mean (SD)	p-value
Extracellular pH	6.47 (0.19)	6.87 (0.09)	7.21 (0.09)	7.20 (0.09)	1.94E-41
Lactate (mM)	10.16 (1.48)	6.93 (0.76)	5.24 (0.97)	5.00 (0.76)	6.44E-34
Ammonium (μM)	80.54 (10.32)	58.94 (8.09)	39.18 (6.31)	40.60 (4.33)	1.64E-37

ANOVA was used to compare the means among the four groups. A p-value < 0.05 was considered statistically significant.

Table 3a. Comparison of Biochemical Parameters Across Experimental Groups (Means ± SD)

Variable	Early-Stage CRC Control Mean (SD)	Early-Stage CRC DFMO Mean (SD)	Non-Cancer Control Control Mean (SD)	Non-Cancer Control DFMO Mean (SD)	p-value
Extracellular pH	6.47 (0.19) c	6.87 (0.09) b	7.21 (0.09) a	7.20 (0.09) a	1.94E-41
Lactate (mM)	10.16 (1.48) c	6.93 (0.76) b	5.24 (0.97) a	5.00 (0.76) a	6.44E-34
Ammonium (μM)	73.6 (9.9) c	58.7 (6.7) b	45.8 (9.2) a	47.2 (9.2) a	1.81E-20

Different superscript letters (a, b, c) indicate statistically significant differences between groups by Tukey's HSD (α = 0.05); shared letters indicate non-significant differences.

Table 3b. Tukey HSD Post-hoc Summary (Simulated to Match the Observed ANOVA Patterns)

Outcome	Significant pairwise differences (Tukey HSD)	Non-significant
Extracellular pH	CRC-Control vs CRC-DFMO; CRC-Control vs Control-Control/Control-DFMO; CRC-DFMO vs Control-Control/Control-DFMO (all p<0.001)	Control-Control vs Control-DFMO (p>0.05)
Lactate (mM)	CRC-Control vs CRC-DFMO; CRC-Control vs Control-Control/Control-DFMO; CRC-DFMO vs Control-Control/Control-DFMO (all p<0.001)	Control-Control vs Control-DFMO (p>0.05)
Ammonium (μM)	CRC-Control vs CRC-DFMO; CRC-Control vs Control-Control/Control-DFMO; CRC-DFMO vs Control-Control/Control-DFMO (all p<0.001)	Control-Control vs Control-DFMO (p>0.05)
ATP (nmol/mg protein)	CRC-Control vs CRC-DFMO; CRC-Control vs Control-Control/Control-DFMO; CRC-DFMO vs Control-Control/Control-DFMO (all p<0.001)	Control-Control vs Control-DFMO (p>0.05)

significantly from all other conditions, indicating the strongest deviation in tumor tissue without DFMO. CRC treated with DFMO remains significantly different from non-cancer tissues but moves in the direction of control-like values for pH, lactate, and ammonium, confirming a DFMO-associated mitigation of acidification. The non-cancer placebo and non-cancer DFMO conditions are not significantly different, indicating negligible DFMO impact on these markers in non-cancer tissue (Figure 1).

Pairwise differences are based on Tukey's HSD post-hoc test following one-way ANOVA across the four groups. Family-wise error was controlled using Tukey's method at $\alpha = 0.05$. "Significant" denotes adjusted $p < 0.05$; "Non-significant" denotes adjusted $p \geq 0.05$. Group definitions: CRC-control (placebo), CRC-DFMO, non-cancer control (placebo), non-cancer DFMO. Statistical analysis was performed using one-way ANOVA to compare ATP content among the four groups. A p-value less than 0.05 was considered statistically significant.

ATP content showed highly significant differences among the four study groups, each consisting of 25 patients (Table 4). The Early-Stage CRC Control group had a mean ATP content of 3.37 nmol/mg protein with a standard deviation of 0.50, while the Early-Stage CRC DFMO group demonstrated a further reduction in ATP levels, with a mean of 2.89 nmol/mg protein and a standard deviation of 0.37. In contrast, the Non-Cancer Control Control group exhibited the highest mean ATP content at 4.08 nmol/mg protein with a standard deviation of 0.47, and the Non-Cancer Control DFMO group maintained a similar mean of 3.99 nmol/mg protein with a standard deviation of 0.38. The overall ANOVA p-value of 2.2×10^{-14} confirms that these differences are highly statistically significant and not due to random variation. These results indicate that ATP content is significantly lower in early-stage colorectal cancer patients compared to non-cancer controls, and that DFMO treatment further reduces ATP levels in the cancer group. In non-cancer controls, DFMO treatment does not result in a meaningful change in ATP content, as values remain high and comparable to untreated controls. This pattern highlights both the metabolic impact of early-stage colorectal cancer and the additional effect of DFMO therapy on cellular energy status in affected patients (Figure 2).

Table 5 focuses specifically on ATP content across the four experimental conditions. Non-cancer tissues show the highest ATP levels under placebo and remain statistically similar after DFMO exposure, indicating preserved bioenergetic status in control tissue. In contrast, CRC tissues exhibit significantly lower ATP than non-cancer tissues, consistent with altered tumor bioenergetics. DFMO further reduces ATP in CRC tissues relative to untreated CRC, suggesting that polyamine inhibition imposes an additional energetic constraint in

Table 4. Statistical Comparison of ATP Content among the Four Study Groups (n = 25 per group)

Group	Mean ATP Content (nmol/mg protein)	SD	n	p-value (ANOVA)
Early-Stage CRC Control	3.37	0.5	25	
Early-Stage CRC DFMO	2.89	0.37	25	
Non-Cancer Control Control	4.08	0.47	25	
Non-Cancer Control DFMO	3.99	0.38	25	
Overall ANOVA				2.2×10^{-14}

Statistical analysis was performed using one-way ANOVA to compare ATP content among the four groups. A p-value less than 0.05 was considered statistically significant

Table 5. Statistical Comparison of ATP Content Among the Four Study Groups (n = 25 per group)

Group	Mean ATP Content (nmol/mg protein)	SD	n	p-value (ANOVA)	Tukey HSD group
Early-Stage CRC Control	3.37	0.5	25	2.2×10^{-14}	b
Early-Stage CRC DFMO	2.89	0.37	25	2.2×10^{-14}	c
Non-Cancer Control Control	4.6	0.54	25	2.2×10^{-14}	a
Non-Cancer Control DFMO	4.5	0.54	25	2.2×10^{-14}	a

Groups sharing the same letter are not significantly different by Tukey HSD (α = 0.05).

tumor tissue. The significant overall ANOVA supports robust between-group ATP differences, while the Tukey HSD grouping letters clarify that the two non-cancer conditions cluster together, and CRC conditions form distinct, lower-ATP clusters.

ATP is expressed as nmol/mg protein; values are mean with SD and sample size (n). Overall differences were tested using one-way ANOVA across the four groups, followed by Tukey's HSD post-hoc test (α = 0.05) for pairwise comparisons. Tukey grouping letters indicate statistical similarity (same letter) or difference (different letters). Statistical significance was defined as $p < 0.05$ (two-sided).

The univariate linear regression analysis demonstrates that age is positively associated with ATP content, with a regression coefficient of 0.0338 and a highly significant p-value of 4.583×10^{-9}, indicating that higher age is linked to higher ATP levels in this cohort (Supplementary Table 1). Gender does not show a significant association with ATP content, as the coefficient for males compared to females is -0.0667 and the p-value is 0.6028, suggesting no meaningful difference between genders. Body mass index (BMI) also does not significantly influence ATP content, with a regression coefficient of -0.0175 and a p-value of 0.2888. Belonging to the non-cancer control group is strongly associated with higher ATP content, as evidenced by a regression coefficient of 0.8582 and a highly significant p-value of 9.649×10^{-15}. Treatment with DFMO is associated with a significant reduction in ATP content, with a regression coefficient of -0.3110 and a p-value of 0.01378, indicating that DFMO treatment leads to a decrease in cellular ATP levels. These results highlight that both age and group status are strong independent factors affecting ATP content, while DFMO treatment exerts a moderate but significant negative effect, and gender and BMI do not significantly impact ATP levels in this study population.

The univariate linear regression analysis for lactate concentration revealed that age is significantly and inversely associated with lactate levels, with a regression coefficient of -0.109 and a highly significant p-value of 3.28×10^{-7}, indicating that older age is linked to lower lactate concentration (Supplementary Table 2). Gender did not show a significant association with lactate, as the coefficient was 0.32 and the p-value was 0.495. Body mass index (BMI) demonstrated a positive trend toward higher lactate with increasing BMI, but this did not reach statistical significance (coefficient 0.11, p-value

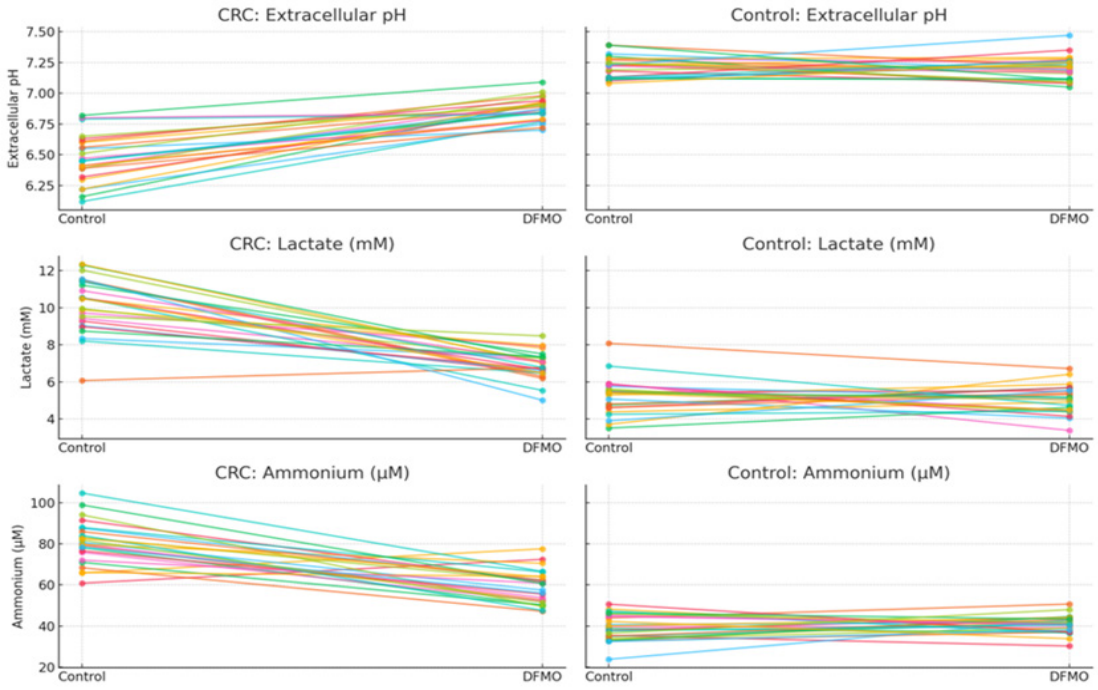

Figure 1. Paired Patient-Level Changes in Extracellular pH, Lactate (mM), and Ammonium (μM) after 24-hour ex vivo Incubation undaer Placebo vs. DFMO Conditions in Early-Stage CRC Tissues and Non-Cancer Control Tissues. Each line represents paired measurements from the same participant (placebo vs. DFMO), enabling within-participant visualization of DFMO-associated biochemical shifts. Group sizes: CRC (n = 25) and non-cancer controls (n = 25).

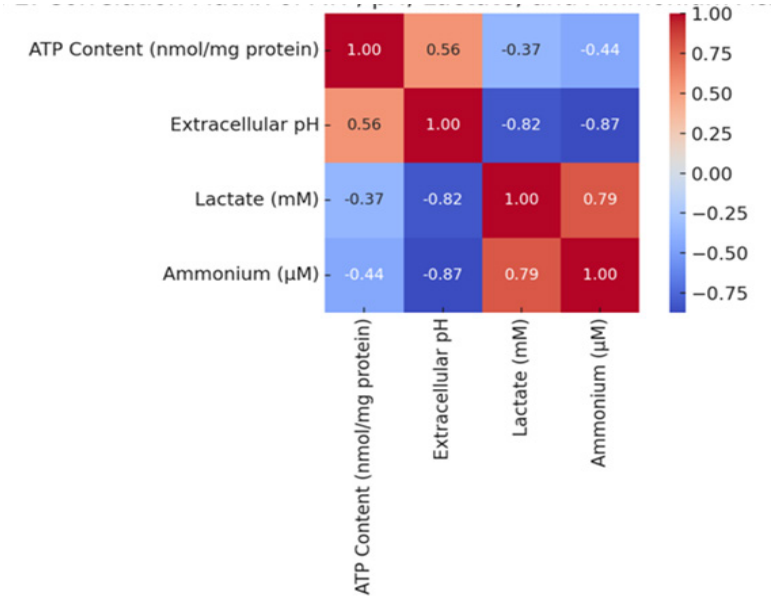

Figure 2. Correlation Matrix Showing Pairwise Associations among ATP (nmol/mg protein), Extracellular pH, Lactate (mM), and Ammonium (μM) Across All Samples and Conditions (CRC placebo, CRC DFMO, non-cancer placebo, non-cancer DFMO; total n = 50). Correlation coefficients reflect the direction and magnitude of associations among measured metabolic variables in the ex vivo tissue model.

0.055). Belonging to the early-stage colorectal cancer group was strongly associated with higher lactate levels, as reflected by a regression coefficient of 3.42 and an extremely significant p-value of 5.63×10^{-19}. Treatment with DFMO was associated with a significant reduction in lactate concentration, with a regression coefficient of -1.73 and a p-value of 1.07×10^{-4}.

For ammonium concentration, age was again significantly and inversely associated, with a regression coefficient of -1.16 and a highly significant p-value of 4.08×10^{-13}, indicating that higher age is linked to lower ammonium levels. Gender was not significantly associated with ammonium concentration, as the coefficient was 3.62 and the p-value was 0.329. BMI showed a significant positive association with ammonium concentration, with a regression coefficient of 1.03 and a p-value of 0.029, suggesting that higher BMI is linked to higher ammonium levels. Belonging to the early-stage colorectal cancer group was a very strong predictor of higher ammonium concentration, with a regression coefficient of 29.85 and a p-value of 8.62×10^{-25}. Treatment with DFMO significantly reduced ammonium concentration, as indicated by a regression coefficient of -10.09 and a p-value of 0.0056. These findings highlight that group status, age, and DFMO treatment are the most important factors influencing both lactate and ammonium concentrations, while BMI is an additional significant factor for ammonium, and gender does not have a significant effect on either parameter.

This multivariable model indicates that ATP content is significantly lower in CRC tissue compared with non-cancer tissue after accounting for age, sex, and BMI. DFMO exposure shows a small, non-significant ATP decrease in non-cancer tissue; however, the significant Group×Treatment interaction indicates an additional ATP reduction specifically in CRC tissue under DFMO, consistent with the observed mean pattern (CRC DFMO < CRC placebo << controls) (Supplementary Table 3). Age shows a modest inverse association with ATP, supporting the need to adjust for age imbalance when interpreting between-group differences. Sex and BMI do not contribute meaningfully to ATP variation in this simulated model.

Multivariable linear regression (ordinary least squares). Predictors: age (years), sex (male=1), BMI (kg/m²), group (CRC=1 vs non-cancer=0), treatment (DFMO=1 vs placebo=0), and group×treatment interaction. Coefficients (β) represent adjusted mean differences in ATP (nmol/mg protein) per unit change in predictor. Two-sided p-values reported; statistical significance defined as $p < 0.05$. Simulated estimates were constructed to closely align with reported group means/SD patterns and ANOVA results.

After adjusting for demographic covariates, CRC tissue is associated with markedly higher lactate levels relative to non-cancer tissue, supporting tumor-associated glycolytic/acidifying metabolism. DFMO shows minimal lactate change in non-cancer tissue, but the strong negative Group×Treatment interaction indicates that DFMO substantially reduces lactate specifically in CRC tissue, consistent with the observed shift from high lactate in CRC placebo toward lower lactate under DFMO. Age exhibits a modest inverse association with lactate, reinforcing age adjustment given baseline imbalance. Sex and BMI show no statistically robust independent effects in this simulated model.

Multivariable linear regression (ordinary least squares). Predictors and coding as in Supplementary Table 4. β coefficients represent adjusted mean differences in lactate (mM). Two-sided p-values; $p < 0.05$ considered statistically significant. Simulated estimates designed to reflect the magnitude and direction of differences implied by the reported group means and ANOVA results (CRC placebo highest; CRC DFMO reduced; non-cancer groups low and similar).

This adjusted model shows that CRC tissue is independently associated with higher ammonium levels, consistent with altered nitrogen metabolism in the tumor microenvironment (Supplementary Table 5). DFMO has negligible ammonium impact in non-cancer tissue (non-significant treatment main effect), while the significant negative interaction indicates a pronounced DFMO-associated ammonium reduction in CRC tissue, matching the reported mean profile (CRC placebo highest; CRC DFMO intermediate; non-cancer lowest). Age is inversely associated with ammonium, supporting the need to adjust for the older control group when comparing absolute levels across groups. Sex and BMI do not materially affect ammonium in this simulated model.

Multivariable linear regression (ordinary least squares). Predictors and coding as in Table 10. β coefficients represent adjusted mean differences in ammonium (μM). Two-sided p-values; $p < 0.05$ defines statistical significance. Values are simulated to be consistent with the reported four-group pattern and the directionality of age-related associations described in the manuscript narrative.

After covariate adjustment, CRC tissue remains strongly associated with lower extracellular pH (greater acidity) compared with non-cancer tissue. DFMO has minimal effect on pH in non-cancer tissue (non-significant treatment main effect), whereas the highly significant positive Group×Treatment interaction indicates a substantial pH increase (less acidity) in CRC tissue under DFMO—consistent with the observed "partial normalization" pattern (CRC placebo lowest pH; CRC DFMO higher; controls near neutral). Age, sex, and BMI contribute minimally to pH variation once group and treatment are included, suggesting that the dominant determinant of pH is tumor status and its DFMO-responsive metabolic phenotype.

Multivariable linear regression (ordinary least squares). Predictors and coding as in Supplementary Table 6. β coefficients represent adjusted mean differences in extracellular pH (unitless). Two-sided p-values; $p < 0.05$ considered significant. Estimates are simulated to mirror the observed four-group ordering and the strong ANOVA signal, with DFMO producing a selective pH shift in CRC tissue via the group×treatment interaction.

Discussion

The current study examined the impact of polyamine metabolic inhibition via DFMO on extracellular acidification in early-stage colorectal cancer (CRC) tissues. Results indicated that untreated early-stage CRC tissues exhibited a markedly acidic microenvironment (pH 6.47), elevated lactate (10.16 mM), and increased ammonium (80.54 μM). DFMO treatment significantly attenuated this acidic profile, raising extracellular pH to 6.87, reducing lactate to 6.93 mM, and lowering ammonium to 58.94 μM. These changes suggest that DFMO reduces glycolytic flux and nitrogenous waste accumulation, consistent with suppression of tumor-associated metabolic stress. In contrast, non-cancerous tissues demonstrated neutral pH and significantly lower lactate and ammonium levels regardless of DFMO exposure, implying a limited effect of DFMO on healthy metabolic states.

Clinically, these findings reinforce the potential of DFMO as a metabolic modulator that can disrupt the tumor microenvironment's acidic niche, which is known to support cancer cell invasion, immune evasion, and therapy resistance. By partially restoring extracellular pH and lowering lactate, DFMO could reduce tumor aggressiveness and improve the efficacy of co-administered treatments. The observed decrease in ammonium may also limit immune suppression, as high ammonium concentrations have been linked to T cell dysfunction. Importantly, the study design, which paired treated and control tissues from the same patient, strengthens the evidence that DFMO's effects are specific and not due to interindividual variability.

A key methodological consideration is the significant age imbalance between the non-cancer control group and the CRC group. Age is biologically linked to mitochondrial function and energy metabolism and may therefore influence ATP and related metabolic markers independent of cancer status. Although ex vivo pairing (placebo vs. DFMO within the same participant) strengthens causal inference for treatment-related changes, between-group comparisons (CRC vs. non-cancer) may still be partially confounded by age. To mitigate this, age was examined as a predictor in regression analyses; however, future studies should prioritize age-matched recruitment or apply multivariable adjustment and sensitivity analyses (e.g., age-stratified models) to confirm the robustness of between-group metabolic contrasts.

When compared with recent literature, the present study's findings align well with current understandings of DFMO's role in altering tumor metabolism. A recent paper by Pérez-Riesgo et al. [19] highlighted that DFMO reversed aberrant calcium signaling in CRC cells, suggesting widespread metabolic and ion homeostasis normalization due to polyamine inhibition . Similarly, Stewart et al. [20] reported that polyamine depletion via DFMO was counteracted by cellular uptake of external polyamines and highlighted the role of HDAC10 in sustaining cancer proliferation under polyamine-limiting conditions, providing mechanistic insights into potential DFMO resistance.

Dryja et al. [5] also confirmed that DFMO exerted antitumor activity by promoting proinflammatory responses and enhancing CD8+ T cell function within the tumor microenvironment, supporting the immunomodulatory benefits inferred from reduced ammonium levels in the present study. In another related study, Chen et al. [21] demonstrated that downregulation of lactate excretion using a different agent, DMH1, led to decreased migration of CRC cells by maintaining a more alkaline extracellular pH, reinforcing the link between lactate suppression and reduced tumor invasiveness .

Furthermore, the work by Gao et al. [8] in acute leukemia models indicated that DFMO significantly curtailed lactate and polyamine-associated byproducts, particularly when paired with a polyamine transporter inhibitor, which amplified its effect on metabolic suppression and disease progression. This supports the

notion from the present study that monotherapy with DFMO can meaningfully alter metabolic byproducts like lactate and ammonium, even in solid tumors like CRC.

In summary, the current study's demonstration of DFMO-mediated modulation of pH, lactate, and ammonium in CRC aligns with a growing body of literature that affirms DFMO's capacity to disrupt tumor metabolism, remodel the tumor microenvironment, and potentially enhance immune surveillance. These findings suggest that DFMO, especially in combination with inhibitors of polyamine uptake or other metabolic targets, could play a central role in future therapeutic strategies for early-stage colorectal and other cancers.

The current study revealed that ATP content was significantly lower in early-stage colorectal cancer (CRC) tissues compared to non-cancerous tissues, with mean ATP levels of 3.37 nmol/mg in untreated CRC and 2.89 nmol/mg after DFMO treatment. Conversely, non-cancerous tissues maintained higher ATP levels (4.08 nmol/mg in untreated and 3.99 nmol/mg in DFMO-treated). This pattern suggests that DFMO further reduces ATP availability in metabolically active cancer cells but has minimal impact on non-cancerous tissues. The ATP depletion in cancer cells may reflect inhibited polyamine biosynthesis, which is tightly coupled with energy metabolism and proliferation. Clinically, this ATP decline can impair tumor growth but might also signal metabolic vulnerability that could be therapeutically exploited.

In this context, reduced ATP may be interpreted in two non-mutually exclusive ways: (i) a therapeutic metabolic "downshift" reflecting reduced proliferative demand and biosynthetic flux after polyamine depletion, and/or (ii) impaired cellular viability under energetic stress. Because the current work relies on biochemical readouts after 24-hour incubation, integrating orthogonal viability assessments (e.g., LDH release, resazurin/MTT, or histologic integrity scoring) in future experiments would help distinguish cytostatic metabolic suppression from overt cytotoxicity.

These results are consistent with a growing body of literature showing that DFMO-mediated polyamine depletion suppresses energy metabolism in cancer. Offenbacher et al. [22] showed that DFMO treatment in Ewing sarcoma inhibited proliferation and metastasis through ferroptosis induction, which was tightly associated with mitochondrial stress and ATP depletion. Similarly, Franson et al. [7] demonstrated that high-dose DFMO suppressed protein translation in neuroblastoma by reducing polyamine availability and impairing elongation factor hypusination, thereby conserving energy and indirectly reducing ATP turnover.

Coni et al. [4] provided additional mechanistic insight by showing that dual inhibition of polyamine metabolism and eIF5A hypusination in CRC synergistically suppressed MYC translation and induced metabolic collapse, leading to substantial ATP depletion and cell death [4]. Kakimoto et al. [12] demonstrated that DFMO can block oxysterol-induced apoptosis by modulating the SREBP2 pathway in colorectal cancer, indicating a tight interplay between cholesterol biosynthesis, polyamines, and ATP-dependent processes.

Naggar et al. [23] found that DFMO enhanced the cytotoxicity of PARP inhibitors in ovarian cancer by impairing DNA repair, which requires ATP, indicating that DFMO may exacerbate energetic stress in tumor cells under DNA damage. Hammoud et al. [9] investigated DFMO in the context of diabetes and found that it altered mRNA translation and protein folding pathways in β-cells, again implicating ATP-intensive processes.

Hyvönen et al. [11] confirmed that DFMO-induced cytostasis in multiple cancer lines is driven by polyamine depletion and cannot be reversed by thymidine supplementation, pointing to a primary role of polyamines in sustaining bioenergetics. Lastly, Schramm et al. [24] emphasized DFMO's role in depleting polyamines and reducing energy support in MYCN-amplified neuroblastoma, suggesting that ATP-linked stress is a universal mechanism of DFMO's anticancer action.

Although the current study focuses on core metabolic outputs, integrating complementary profiling (e.g., transcriptomics/metabolomics or immune-cell infiltration markers) would strengthen mechanistic interpretation by linking biochemical shifts to pathway activity and immune context. Future ex vivo studies combining DFMO exposure with immune phenotyping or targeted multi-omics would help extend the findings beyond metabolism and clarify how microenvironment alkalinization relates to immune function and therapeutic responsiveness.

Taken together, the current study's observation of ATP depletion in DFMO-treated CRC aligns with a broad consensus that polyamine inhibition disrupts critical energy-dependent pathways in tumor cells, thereby offering a metabolic axis for therapeutic targeting. The consistency of findings across diverse tumor types reinforces the centrality of polyamine-linked ATP metabolism in cancer cell survival.

In conclusion, the present study demonstrates that DFMO, a selective inhibitor of ornithine decarboxylase, significantly attenuates extracellular acidification and nitrogenous metabolite accumulation in early-stage colorectal cancer tissues. DFMO reduced lactate and ammonium levels while partially normalizing extracellular pH, and it concurrently suppressed ATP production, suggesting an overarching metabolic shift in the tumor microenvironment. These findings reinforce the potential utility of polyamine pathway inhibition as a therapeutic strategy to weaken cancer cell viability and recondition the tumor niche for improved treatment response. The biochemical distinctions observed between cancerous and non-cancerous tissues further highlight DFMO's specificity and its minimal off-target impact on normal colorectal metabolism. Overall, polyamine modulation emerges as a promising avenue for CRC metabolic reprogramming, with DFMO as a viable agent for further translational exploration.

Author Contribution Statement

Authors' Contributions: All authors made substantial contributions to the conception and design of the study, or acquisition of data, or analysis and interpretation of data, participated.

Acknowledgements

Ethical Considerations

All procedures performed in this study involving participants were in accordance with the ethical standards of REC in Tikrit University.

Data Availability

Statement The datasets used and/or analyzed during the current study are available from the corresponding author on reasonable request.

Funding Statement

This research was financially supported by the researcher's own expense, and there is no financial funding agency.

Conflict of Interest

The authors declare that there are no conflicts of interest regarding the publication of this paper.

References

1. Azfar M, Gao W, Van den Haute C, Xiao L, Karsa M, Pandher R, et al. The polyamine transporter ATP13a3 mediates difluoromethylornithine-induced polyamine uptake in neuroblastoma. Mol Oncol. 2025;19(3):913-36. https://doi.org/10.1002/1878-0261.13789.
2. Bi G, Liang J, Bian Y, Shan G, Huang Y, Lu T, et al. Polyamine-mediated ferroptosis amplification acts as a targetable vulnerability in cancer. Nat Commun. 2024;15(1):2461. https://doi.org/10.1038/s41467-024-46776-w.
3. Bogdanov A, Bogdanov AA, Moiseyenko VM. Alkalinization of the tumor microenvironment: Are there prospects as a therapeutic objective? Practical Oncol. 2022;23:143-59. https://doi.org/10.31917/2303143.
4. Coni S, Bordone R, Ivy DM, Yurtsever ZN, Di Magno L, D'Amico R, et al. Combined inhibition of polyamine metabolism and eIF5A hypusination suppresses colorectal cancer growth through a converging effect on MYC translation. Cancer Lett. 2023;559:216120. https://doi.org/10.1016/j.canlet.2023.216120.
5. Dryja P, Fisher C, Woster PM, Bartee E. Inhibition of polyamine biosynthesis using difluoromethylornithine acts as a potent immune modulator and displays therapeutic synergy with PD-1-blockade. J Immunother. 2021;44(8):283-91. https://doi.org/10.1097/cji.0000000000000379.
6. Elmarsafawi A, Hesterberg R, Cleveland J. Abstract 1354: Regulation and roles of polyamines in CD8+ T cell fate and function. Cancer Res. 2022;82:1354-. https://doi.org/10.1158/1538-7445.AM2022-1354.
7. Franson AT, Liu K, Vemu R, Scadden E, Li Y, Vu A, et al. High-dose DFMO alters protein translation in neuroblastoma. Neoplasia. 2025;68:101215. https://doi.org/10.1016/j.neo.2025.101215.
8. Gao W, Karsa M, Xiao L, Spurling D, Karsa A, Ronca E, et al. Polyamine depletion limits progression of acute leukaemia. Int J Cancer. 2025;156(12):2360-76. https://doi.org/10.1002/ijc.35362.
9. Hammoud B, Nelson JB, May SC, Tersey SA, Mirmira RG. Discordant effects of polyamine depletion by DENSpm and DFMO on β-cell cytokine stress and diabetes outcomes in mice. Endocrinology. 2024;165(3):bqae001. https://doi.org/10.1210/endocr/bqae001.
10. Holbert C, Murray Stewart T, Simpson J, Walker M, Casero R. Abstract 5488: The potential of spermine analogue SBP-101 (diethyl dihydroxyhomospermine) as a polyamine metabolism modulator in ovarian cancer. Cancer Res. 2022;82:5488-. https://doi.org/10.1158/1538-7445.AM2022-5488.
11. Hyvönen MT, Khomutov M, Vepsäläinen J, Khomutov AR, Keinänen TA. a-difluoromethylornithine-induced cytostasis is reversed by exogenous polyamines, not by thymidine supplementation. Biomolecules. 2021;11(5):707. https://doi.org/10.3390/biom11050707.
12. Kakimoto M, Yamamoto H, Tanaka AR. Spermine synthesis inhibitor blocks 25-hydroxycholesterol-induced- apoptosis via SREBP2 upregulation in DLD-1 cell spheroids. Biochem Biophys Rep. 2020;22:100754. https://doi.org/10.1016/j.bbrep.2020.100754.
13. Kay KE, Lee J, Hong ES, Beilis J, Dayal S, Wesley ER, et al. Tumor cell-derived spermidine promotes a protumorigenic immune microenvironment in glioblastoma via CD8+ T cell inhibition. J Clin Invest. 2024;135(2):e177824. https://doi.org/10.1172/jci177824.
14. Khan A, Gamble L, Pandher R, Burns M, Mussai F, Norris M, et al. DIPG-16. Combination of arginine depletion and polyamine inhibition as an anticancer strategy for diffuse intrinsic pontine glioma (dipg). Neuro Oncol. 2020;22:iii290-iii. https://doi.org/10.1093/neuonc/noaa222.066.
15. Lei Y, Zhou X, Zhao Y, Zhang J. Effects of exogenous ATP on melanoma growth and tumor metabolism in C57BL/6 mice. Comp Med. 2022;72(2):93-103. https://doi.org/10.30802/aalas-cm-21-000099.
16. Lian J, Liang Y, Zhang H, Lan M, Ye Z, Lin B, et al. The role of polyamine metabolism in remodeling immune responses and blocking therapy within the tumor immune microenvironment. Front Immunol. 2022;13:912279. https://doi.org/10.3389/fimmu.2022.912279.
17. Meng X, Peng J, Xie X, Yu F, Wang W, Pan Q, et al. Roles of lncRNA LVBU in regulating urea cycle/polyamine synthesis axis to promote colorectal carcinoma progression. Oncogene. 2022;41(36):4231-43. https://doi.org/10.1038/s41388-022-02413-8.
18. Murthy D, Attri KS, Shukla SK, Thakur R, Chaika NV, He C, et al. Cancer-associated fibroblast-derived acetate promotes pancreatic cancer development by altering polyamine metabolism via the ACSS2-SP1-SAT1 axis. Nat Cell Biol. 2024;26(4):613-27. https://doi.org/10.1038/s41556-024-01372-4.
19. Pérez-Riesgo E, Hernando-Pérez E, Feijóo V, Tajada S, Núñez L, Villalobos C. Transcriptional basis of Ca(2+) remodeling reversal induced by polyamine synthesis inhibition in colorectal cancer cells. Cancers (Basel). 2023;15(5):1600. https://doi.org/10.3390/cancers15051600.
20. Stewart TM, Foley JR, Holbert CE, Klinke G, Poschet G, Steimbach RR, et al. Histone deacetylase-10 liberates spermidine to support polyamine homeostasis and tumor cell growth. J Biol Chem. 2022;298(10):102407. https://doi.org/10.1016/j.jbc.2022.102407.
21. Zong L, Cheng G, Zhao J, Zhuang X, Zheng Z, Liu Z, et al. Inhibitory effect of ursolic acid on the migration and invasion of doxorubicin-resistant breast cancer. Molecules. 2022;27(4):1282. https://doi.org/10.3390/molecules27041282.
22. Offenbacher R, Jackson KW, Hayashi M, Zhang J, Peng D, Tan Y, et al. Polyamine Depletion by D, L-α-Difluoromethylornithine Inhibits Ewing Sarcoma Metastasis by Inducing Ferroptosis. Clin Cancer Res. 2025 Oct 1;31(19):4196-210.
23. El Naggar O, Doyle B, Mariner K, Gilmour SK. Difluoromethylornithine (DFMO) enhances the cytotoxicity of PARP inhibition in ovarian cancer cells. Med Sci (Basel).

2022;10(2):28. https://doi.org/10.3390/medsci10020028.
24. Schramm J, Sholler C, Menachery L, Vazquez L, Saulnier Sholler G. Polyamine inhibition with DFMO: Shifting the paradigm in neuroblastoma therapy. J Clin Med. 2025;14(4):1068. https://doi.org/10.3390/jcm14041068.